Canadian Nuclear Society
Waste Management, Decommissioning and Environmental Restoration
for Canada's Nuclear Activities: Current Practices and Future Needs
Ottawa, Ontario Canada May 8-11 2005

CONSIDERATION OF ACCIDENT EVENTS DURING ON-SITE WASTE HANDLING

Greg Morandin (a), Eric Araujo (a), Corneliu Manu (b), Richard Sauvé (a)
Fuel Channel and Materials Engineering Branch (a)
ACR Reactor and Fuel Handling Branch (b)
Atomic Energy of Canada Ltd.
2251 Speakman Dr.
Mississauga, Ontario, Canada, L5K 1B2

ABSTRACT

The safe on-site transport of spent nuclear fuel must rely on the structural integrity of the transport container and the system of transport. Regard for safe and efficient on-site transport routes are important and manageable using well thought-out planning. Difficulties arise when non-manageable incidences occur such as flying debris from tornado-force winds that may result in high velocity impact on the transport system. Part of the site Nuclear Safety Design Guide considers design basis tornado (Level F0) incidents. A Dry Storage Container (DSC) is used to transport and store spent fuel. A DSC is loaded with spent fuel and typically travels on-site to a processing building for permanent lid attachment. During on-site transport a lid clamp is utilized to ensure the container lid remains in place. This paper consists of simulations that consider several wind borne projectiles impacting the DSC. These types of postulated accident scenarios are analysed using detailed nonlinear finite element techniques. A state-of-the-art, large deformation, non-linear, finite element code is used in the simulations.

Projectile impact poses two concerns. Large object impact (large poles, piping) in the vicinity of the lid/container interface may result in damage to the lid clamp and dislodging of the lid. Small object impact (slender solid rods) may result in through-wall penetration and loss of shielding. Impact simulation results for these two types of objects show that for large projectiles the lid clamp retains the lid/body interface and for small projectiles there is no penetration of the container wall, ensuring safe containment of spent fuel under tornado conditions.

1. INTRODUCTION

The Used Fuel Dry Storage Facility (UFDSF) at the site of the Darlington Nuclear Generating Station (DNGS) is in the design/planning concept phase. The purpose of the UFDSF is to receive Dry Storage Containers (DSCs) and to prepare the DSCs for transport to the DNGS

irradiated fuel bay where they are loaded with the minimum ten-year-old cooled fuel. A lid clamp is fitted to the DSC and it is then transported on site to the UFDSF where the DSC lid is seal welded and placed in the storage location at the UFDSF. In this capacity the DSC provides secure passive surface storage for used fuel.

In order to ensure the safe transport of the DSC on the site of the DNGS, an assessment of possible damage to the DSC from flying debris during a F0 tornado was performed in fulfilment of licensing qualification. The simulations address the response of the DSC lid-body assembly and transfer clamp due to impacts from debris initially driven by a design basis tornado. This analysis was performed in order to ensure safe spent nuclear fuel containment in a DSC during a F0 tornado event.

In the analyses conducted herein, three-dimensional nonlinear simulations of the postulated accident scenarios described in the foregoing are used to evaluate the response of the DSC to the specified conditions. In the simulations summarised herein, the three-dimensional nonlinear finite element computer code *H3DMAP* [1] was employed.

2. FINITE ELEMENT MODEL OF DSC AND TRANSFER CLAMP

In order to assess the possible damage to the DSC during the postulated accident scenarios, a full-scale, three-dimensional, finite element model was developed with refinement in key areas (Figure 1). The 72,505 kg DSC model is comprised of a high-density concrete body and lid encased in a shell fabricated from CSA G40.21M grade 300WT steel. The lid and body are attached through two flange plates made of 300WT material (Figure 2).

The transfer clamp model (Figure 1) consists of a C-shaped channel section, structurally reinforced with vertical web plates, attached to a solid 82-mm shear skirt. The shear skirt houses a total of 26 cam pivoted clamping dogs (Figure 1) situated along each side of the clamp. When the dogs are engaged they swing under the body flange plate, containing the flange plates between the C-frame and the dogs. The purpose of the simulations is to assure that the integrity of the DSC is not compromised via lid separation or containment penetration, where containment is defined as the sealed inner volume of the DSC.

Table 1 lists the details of the simulation model. Contact surfaces, including a stick/slip formulation are specified between each separate component [1], [2]. In all, there were 31 contact surfaces modeled.

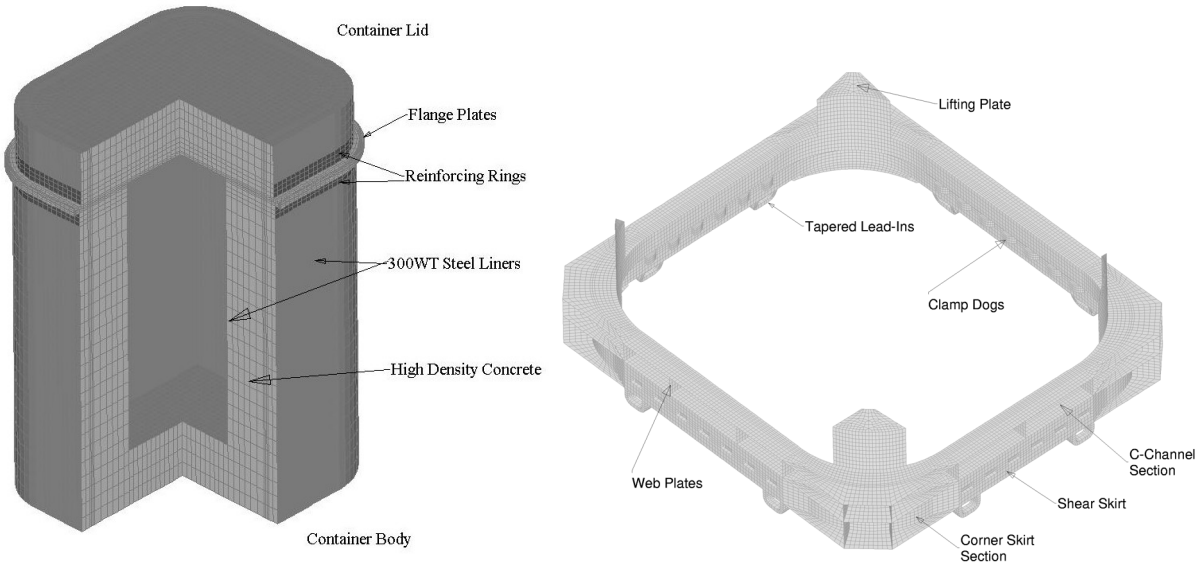

Figure 1 – Dry Storage Container and Transfer Clamp Model

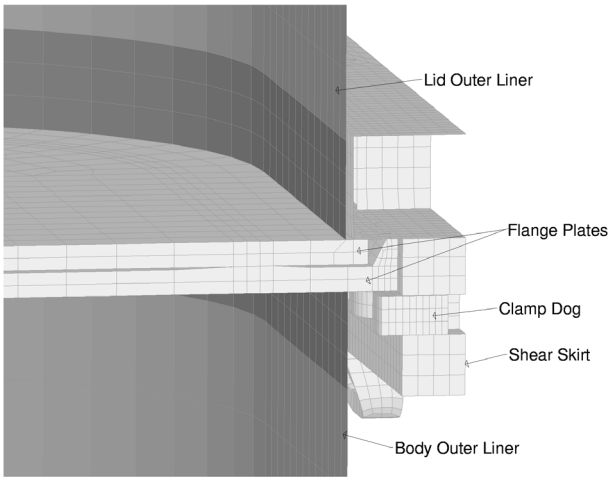

Figure 2 - Section View of Clamp/DSC Assembly

Table 1 - Details of DSC Simulation Model

Model Topology		
Components	Element Formulation	Number of Elements
DSC Shell	3D Shells	10,876
Concrete	3D Continuum	52,184
Lid Flange	3D Continuum	4,504
Body Flange	3D Continuum	5,844
Lid Clamp	3D Shells 3D Continuum	13,850 17,350

3. Projectile Models -Tornado Simulation

3.1. Wood Pole

In reviewing the design basis F0 tornado, the worst-case debris object in terms of impact energy is a utility pole measuring 0.34-m diameter by 10.7-m long and weighing 676 kg. The pole is considered to reach a maximum speed of 46.7 m/s as a result of the tornado. The pole is modelled using 4,800 8-noded, three dimensional continuum elements with wood material properties. No damage to the wood is considered and elastic behaviour is assumed as this provides a conservative upper bound assessment (i.e., all damage must be incurred by the DSC/Lid Clamp assembly).

3.2. Steel Pipe

The second critical debris object considered is a 0.3-m diameter schedule 40 pipe measuring 4.6-m long and weighing 337 kg. The pipe velocity arising from the forces of the tornado is estimated to be 46.7 m/s. The pipe is modelled using a total of 7,200, 4-noded shell elements with elastic-plastic carbon steel material properties. A three dimensional single surface contact model is used in conjunction with the general arbitrary contact model to account for the possibility that the shell folds on itself during the expected severe deformation.

3.3. Solid Rod

The final critical debris object considered is a 25.4-mm diameter solid rod measuring 0.9-m long and weighing 3.6 kg. The tornado is assumed to induce a velocity to the rod of 69.7 m/s. Since the impact is very localized and refinement is required to capture possible damage, a partial slab model is used to represent the wall of the DSC. The partial slab model consists of 43,200, 8-noded, three dimensional continuum elements used to discretize the concrete wall and 7200, 4-noded shell elements for modelling the inner and outer steel liners. The rod is modelled using 2400, 8-noded continuum elements with elastic-plastic carbon steel material constitutive relation. The finite element model of the partial DSC slab and steel rod is shown in Figure 3.

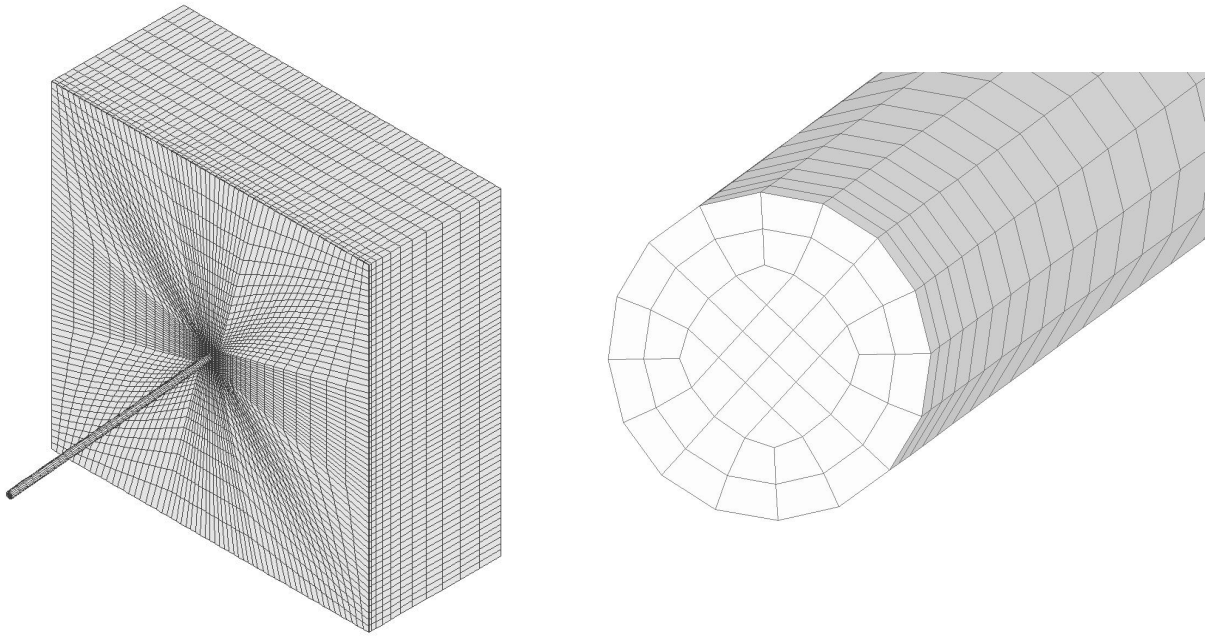

Figure 3 – Rod Impact Slab Model

4. MATERIAL MODELS

The materials are assumed to be strain rate independent for the purpose of the simulations. This assumption produces conservative estimates of damage, as including strain rate dependant hardening would increase the flow stress and hence reduce the deformation in the DSC.

4.1. CSA G40.21 Grade 300WT Steel

The 300WT steel used for the inner and outer liners of the DSC and the flange plates is modelled using a variable hardening elastic-plastic material. The engineering and idealised stress/strain curves for the material are presented in Figure 4. The remaining material properties used are listed in Table 2.

4.2. ASTM A564 Type 630 Steel Condition 1025

The material used for the clamp dogs is fabricated from ASTM A564 type 630 steel, which is a high strength material [3]. The material is modelled using an isotropic, elastic-plastic constitutive relation including a hardening modulus. The material properties used are listed in Table 2. The material was assumed to be strain rate independent for the purpose of the simulations.

4.3. 304L Stainless Steel

The clamp frame and skirt are constructed from 304L stainless steel [5]. The material is modelled using an isotropic, elastic-plastic constitutive relation including a hardening modulus. The material properties used are listed in Table 2. The material was assumed to be strain rate independent for the purpose of the simulations.

4.4. Tempered Steel Rod

The material used for the rod is a tempered steel. The material is modelled using an isotropic, elastic-plastic constitutive relation including a hardening modulus. The material properties used are listed in Table 2. The material was assumed to be strain rate independent for the purpose of the simulations.

4.5. Concrete

The concrete is modelled as an isotropic-hydrodynamic elastic-plastic material with an equation of state [4]. The pressure versus volumetric strain curve and the yield stress versus pressure relation are shown in Figure 5, respectively. A yield stress of 20 MPa and the pressure/volumetric strain curve were taken from OPG testing data. The yield/pressure curve was estimated from [6]. The material was assumed to be strain rate independent for the purpose of the simulations. The other properties used for concrete are as follows:

Shear Modulus, G = 20,000 MPa

Weight per unit volume = 3,871 kg/m^3

Tensile Cut-off Pressure = -1.4 MPa (negative in tension)

28 Day Compressive Strength = 20 MPa

4.6. Wood

The utility pole is modelled as an isotropic elastic material with wood properties [7]. The material properties used are listed in Table 2. The material was assumed to be strain rate independent for the purpose of the simulations.

Table 2 - Properties of Materials

Material	Weight per Unit Volume (kg/m^3)	Elastic Modulus (MPa)	Poisson's Ratio	Initial Yield Stress (MPa)	Hardening Modulus (MPa)	Effective Plastic Strain Limit
CSA G40.21 Grade 300WT Steel	7,850	203×10^3	0.3	370	True Stress/True Strain Curve	15%
ASTM A564 Type 630 Steel Condition 1025	7,800	200×10^3	0.272	1000	1724	12% [3]
304L Stainless Steel	8,027	193×10^3	0.28	298.5	1,517	20% [5]
Tempered Steel Rod	7,860	200×10^3	0.3	700	2000	-
Concrete	3,871	-	-	-20	-	-
Wood	688	9.31×10^3	0.15	-	-	-

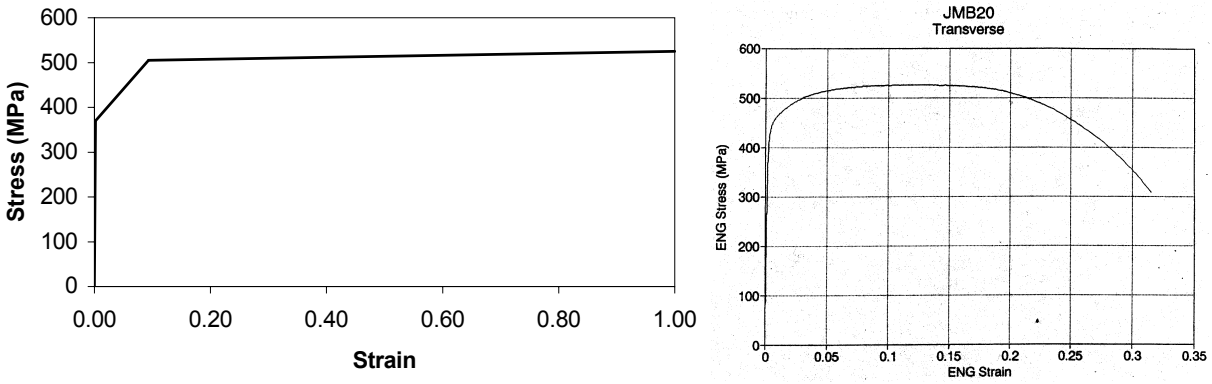

Figure 4 – CSA G40.21 Grade 300WT Steel Idealised and Engineering Stress/Strain Curves

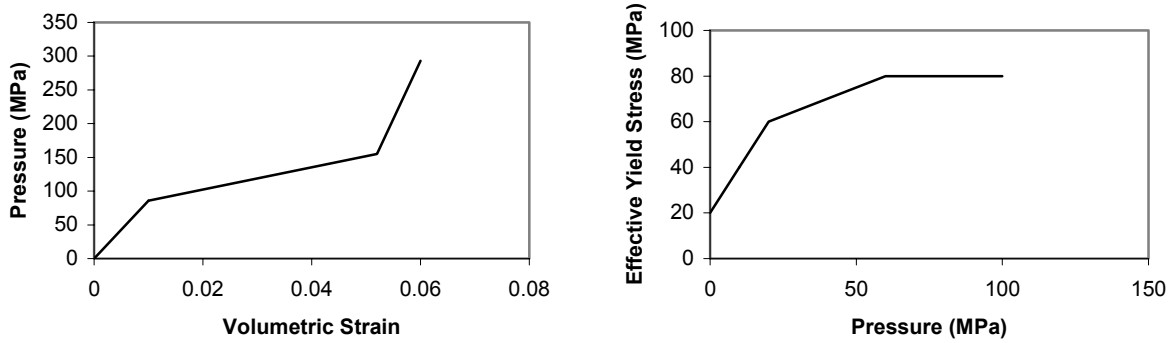

Figure 5 – Concrete Pressure Versus Volumetric Strain Curve and the Yield Stress Versus Pressure Relation

5. SIMULATION CASES

5.1. Tornado Debris Impact

5.1.1. Loading

A review of the design basis F0 tornado was performed, and three tornado-generated missiles and their velocities are listed. The three cases analysed envelope all possible projectiles as defined in the design basis tornado scenario. This assumption was based on projectile type and the kinetic energy at impact as outlined in Table 3.

Table 3 – Tornado Generated Missile Cases

Description	Missile Mass (kg)	Missile Velocity (m/s)	Kinetic Energy (N·m)
Wood Pole	674.0	46.7	734,960
Steel Pipe	336.0	46.7	366,390
Steel Rod	3.6	69.7	8,745

5.1.2. Wood Utility Pole Impact on DSC Lid

The design basis for a tornado considers the possibility of a wood utility pole travelling at 46.7 m/s. The worst-case scenario would be the end of the wood pole impacting the DSC lid squarely on the side of the lid. This bounding impact scenario concentrates all the pole's mass onto the lid, which will try to move the lid off the container body, exposing the contents.

5.1.3. Steel Pipe Impact on DSC Lid

The design basis for a tornado considers the possibility of a steel pipe travelling at 46.7 m/s. This impact modelled at 0° and 5° normal to the lid concentrates the entire pipe mass onto the lid, which will try to move the lid off the container body, exposing the contents.

5.1.4. Solid Rod Impact on DSC Wall

The design basis for a tornado considers the possibility of a solid rod travelling at 69.7 m/s. The worst location for the solid rod to impact would be the sidewall of the DSC where the minimum combined plate thickness is located. This scenario was postulated, as penetration into the containment volume was deemed most likely in this area due to impact by a slender projectile.

5.2. Results

5.2.1. Wood Pole Impact on DSC Lid

The overall deformation due to the wood pole impacting the DSC is evident in Figure 6. The pole impacts the DSC lid squarely imparting all the impact energy to the container and then rebounds off the lid. The impact force pushes the lid across the body flange plate and the lid begins to separate from the container by travelling up the body flange plate lip (Figure 6).

The impact force time-history curve is shown in Figure 7. A maximum impact force of 12 MN occurs at 1.4 ms. This equates to an impact acceleration of 1,817 g. Figure 8, Figure 9, and Figure 10 present the resulting damage to various DSC components. There is a maximum effective plastic strain of 1.65% in the lid liner in the vicinity of the initial impact between the wood pole and the DSC lid. This level of strain is well below the acceptable strain level for 300WT steel, which is approximately 15%.

Damage to the transfer clamp is presented in Figure 9 and Figure 10. There are low levels of plasticity in the clamp skirt around the dog windows. This is a result of the clamping load that is

transferred from the dogs to the skirt. There is also plasticity in the interface plate between the clamp skirt and the upper frame. This is also a result of the clamping interaction with the DSC flange plates and the clamp frame. The maximum localized plasticity found in the clamp dogs was approximately 9% on the edge of one of the dogs. The plastic strain is a result of the compressive load on the edge of the dog.

The damage sustained to the DSC in this scenario was far below the threshold for containment failure, ensuring the safe storage and transport of spent fuel under these conditions.

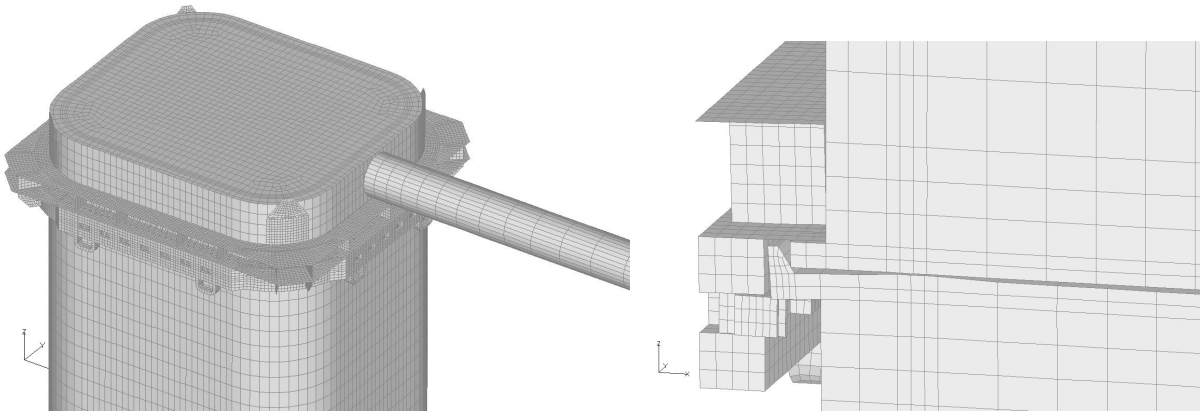

Figure 6 – Overall Deformation at Point of Pole Rebound and Relative Deformation of Flange Plates

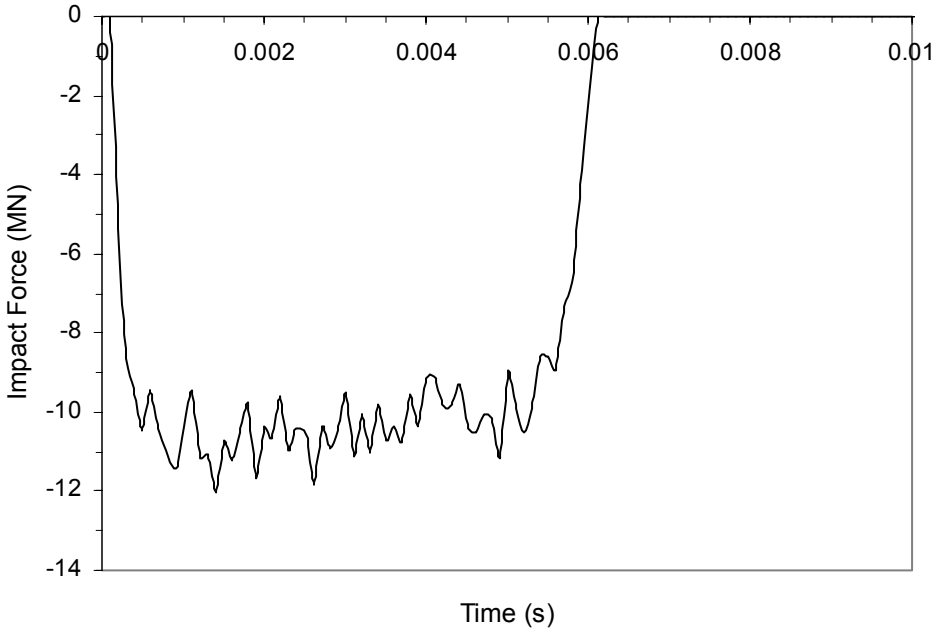

Figure 7 – Impact Force Time-History for Wood Pole Impact

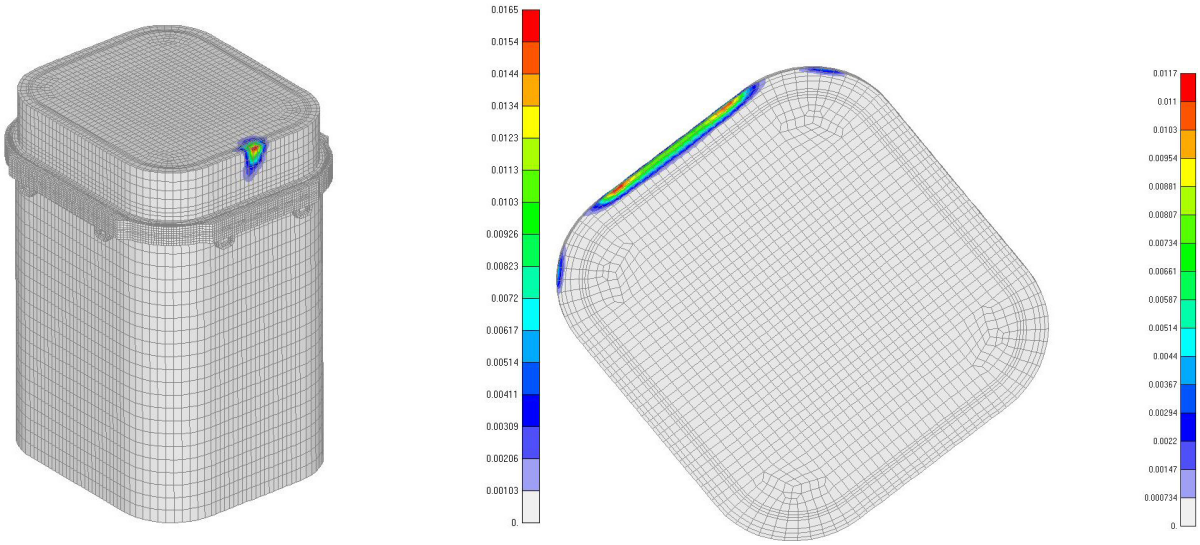

Figure 8 – Effective Plastic Strain in DSC Outer Shell and DSC Lid Flange

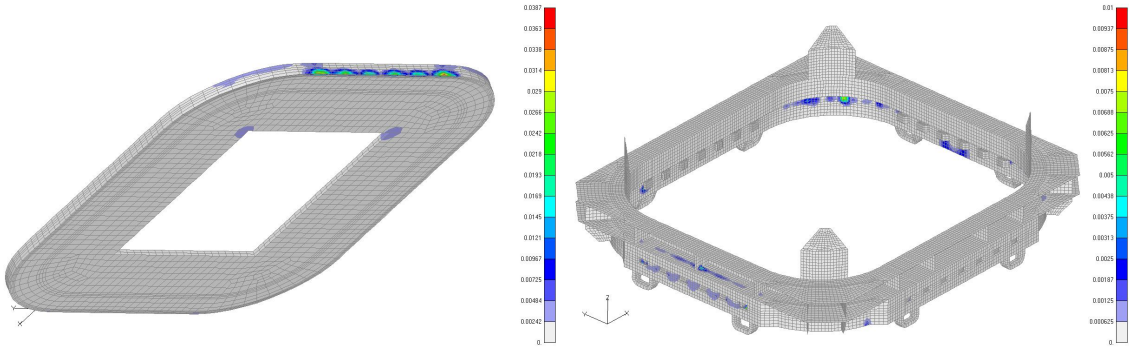

Figure 9 - Effective Plastic Strain in DSC Body Flange and Transfer Clamp Skirt

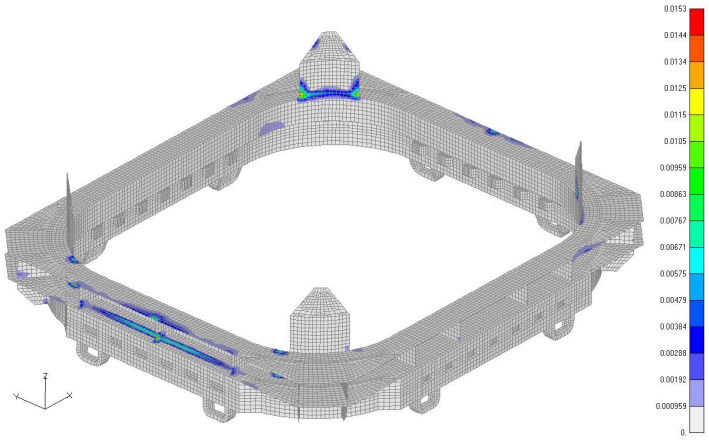

Figure 10 – Effective Plastic Strain in Transfer Clamp Shell

5.2.2. Steel Pipe Impact on DSC Lid

The impact force time-history curves for the normal impact case and the 5° impact case are shown in Figure 11. A maximum impact force of 3.75 MN occurs at 0.5 ms for the normal impact case, which equates to an acceleration load of 1,138 g. A maximum impact force of 2.55 MN occurs at 1.9 ms for the 5° impact case, which equates to an acceleration load of 774 g. Comparison of the total energy input into the DSC lid for both cases is very close. The normal impact case results in a higher peak force and a lower duration compared to the 5° case. Due to the similarity in the results, only the 5° case is presented.

The overall deformation of the steel pipe impacting the DSC is evident in Figure 12. The pipe impacts the DSC lid initially at a 5° angle. The impact causes the end of the pipe to deform and slide across the lid, and then rebound off the lid. The impact force pushes the lid across the body flange plate and the lid begins to separate from the container by travelling up the body flange plate lip. When all the free clearances between the lid and body flanges are reduced, the transfer clamp gets loaded. Figure 12 shows the maximum separation of the two flange plates as the lid flange rides up the body flange lip.

Figure 12 presents the damage to the end of the pipe. The pipe end folds back onto itself to produce a flared end. Figure 13 and Figure 14 present the resulting damage to various DSC components. There is a maximum effective plastic strain of 0.8% in the lid liner in the vicinity of the initial impact between the steel pipe and DSC lid. This level of strain is well below the acceptable strain level for 300WT steel, which is approximately 15%. Damage to the body flange is presented in Figure 13. There are some small levels of plasticity along a corner edge of the body flange resulting from impact (Figure 12) of the lid with the body flange. It is evident from the localized strain that the corner dog takes most of the clamping load. The maximum effective plastic strain of 0.24% is well below the acceptable level for 300WT steel.

Damage to the transfer clamp is presented in Figure 14. There are low levels of plasticity in the clamp skirt around the corner dog window. This is a result of the clamping load that is transferred from the dog to the skirt. There is also plasticity in the vertical clamp plate in the vicinity of initial impact. This is a result of the pipe shell folding back and impacting the clamp frame. There is a localized strain of approximately 0.3% on the edge of the dog. The plastic strain is a result of the compressive load on the edge of the dog.

The damage sustained to the DSC in this scenario was far below the threshold for containment failure, ensuring the safe storage and transport of spent fuel under these conditions.

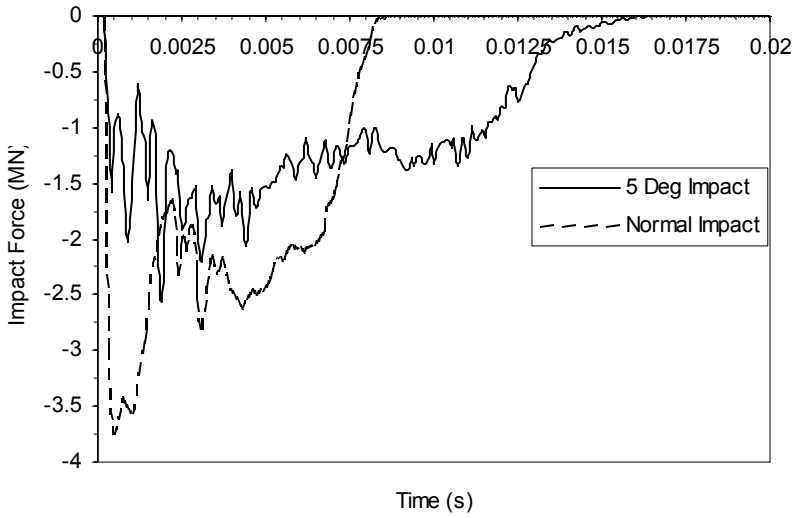

Figure 11 – Impact Force Time-History for Steel Pipe Impact

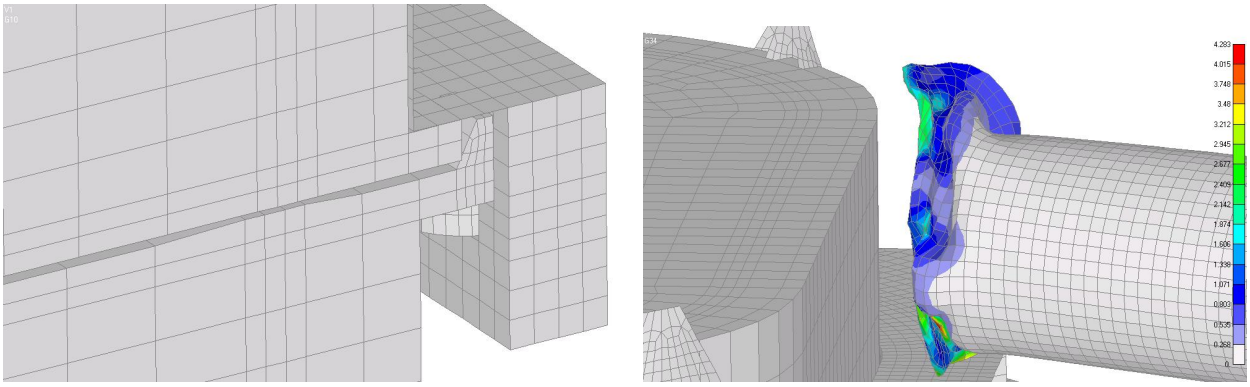

Figure 12 – Relative Deformation of Flange Plates and Predicted Damage to Steel Pipe

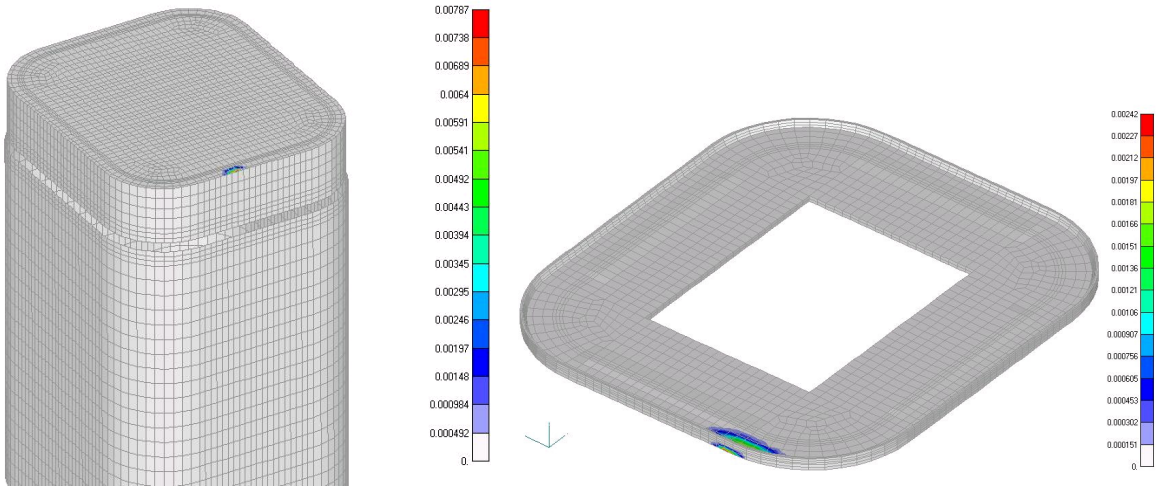

Figure 13 – Effective Plastic Strain in DSC Outer Shell and Body Flange

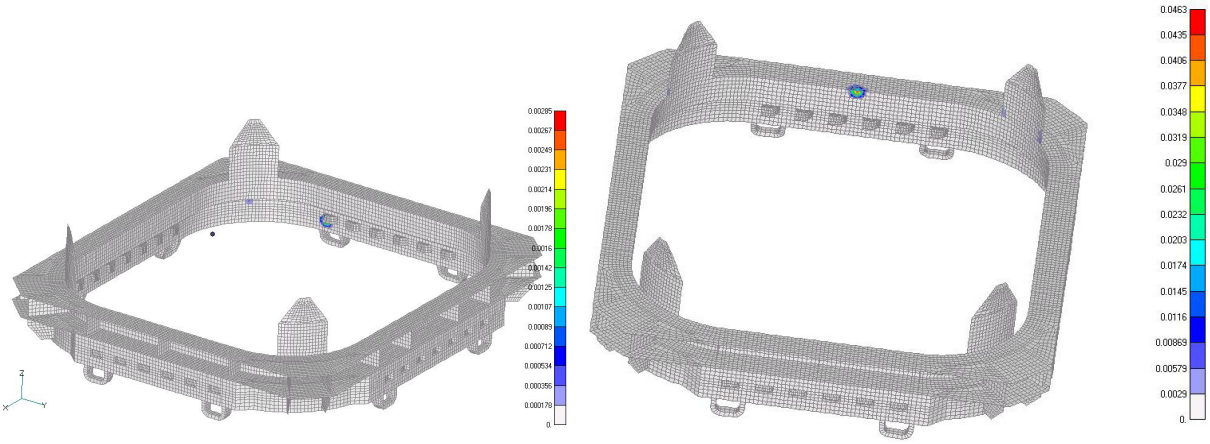

Figure 14 – Effective Plastic Strain in Transfer Clamp Skirt

5.2.3. Steel Rod Impact on DSC Wall

The impact force time history curves for the normal impact case and the 5° impact case are shown in Figure 15. A maximum impact force of 0.5 MN occurs at 0.2 ms for the normal impact case, which equates to an acceleration load of 14,164 g. A maximum impact force of 0.07 MN occurs at 0.6 ms for the 5° impact case, which equates to an acceleration load of 1,983 g. The normal impact case results in a much higher peak force for a similar duration compared to the 5° case; therefore the normal case is presented in this work.

In this simulation, the rod impacts the DSC wall initially and the impact causes the end of the pipe to deform and rebound off the wall. The impact force deforms the outer liner of the container wall and damages the concrete.

Figure 16 presents the effective plastic strain in the outer liner of the DSC wall. A maximum strain of 6.13% occurs in the vicinity of the initial impact. This level of strain is below the allowable plastic strain limit for 300WT steel, which is approximately 15%. The effective plastic strain in the rod is evident in Figure 16. There is a region of high, localized strain (47%) at the impact end of the rod, on the periphery, with evidence of bulging at the rod end. There is no evidence of damage to the inner steel liner of the DSC.

The damage sustained to the DSC in this scenario was far below the threshold for containment failure, ensuring the safe storage and transport of spent fuel under these conditions.

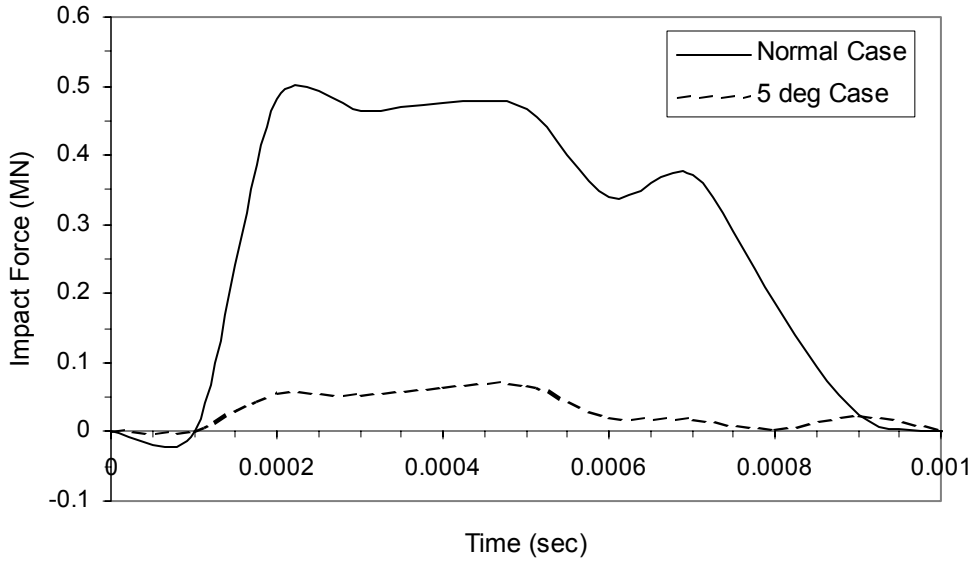

Figure 15 – Impact Force Time History for Steel Rod Impact

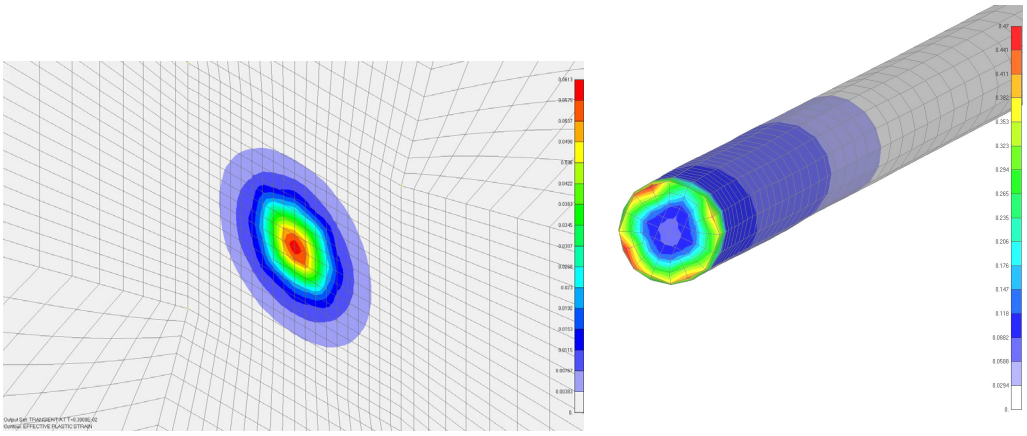

Figure 16 – Effective Plastic Strain in the Outer DSC Plate and in the Steel Rod

6. CONCLUSIONS AND RECOMMENDATIONS

Safe on-site transport of the Dry Storage Container (DSC) at the Darlington Nuclear Generating Station must satisfy a series of postulated accident scenarios due to a projectile impact resulting from tornado force winds.

The requirement covered in this work is the evaluation of the DSC/Lid Clamp integrity under severe environmental conditions (e.g., tornado). Projectile impact onto the DSC due to tornado force winds is considered. A number of projectiles were considered in the simulations. The projectiles considered include a solid wood utility pole, a large diameter steel pipe in various orientations impacting the DSC lid, and a 25.4-mm diameter solid rod impacting a wall of the DSC. Large deformation impact simulations are performed in order to evaluate the structural integrity of the transfer clamp and the DSC assembly.

In all cases the transfer clamp retains the DSC lid with little damage to the container and clamp. The damage sustained to the DSC in these scenarios was far below the threshold for containment failure, ensuring the safe storage and transport of spent fuel under Design Basis tornado conditions.

The penetration simulation of a 25.4-mm diameter steel rod impacting the sidewall of the DSC indicates that the structural integrity of the container wall is not compromised and predictions demonstrate that the outer liner of the DSC is not penetrated. The damage sustained to the DSC in this scenario was far below the threshold for containment failure, ensuring the safe storage and transport of spent fuel under these conditions.

7. ACKNOWLEDGEMENTS

The basis of this work was funded by the client, Ontario Power Generation, and was submitted with permission to publish relevant information.

8. REFERENCES

[1] Sauvé, R.G., *H3DMAP Version 6 – A General Three Dimensional Finite Element Computer Code for Linear and Nonlinear Analyses of Structures – User Documentation,* Ontario Power Technologies Report No. 181.1-H3DMAP-1998-RA-0001-R00, 1999.

[2] Sauvé, R.G., Morandin, G., Khajehpour, S., *Contact Simulation in Finite Deformation – Algorithm and Modelling Issues*, Symposium on Computational Mechanics, ASME PVP-Vol 441, pp. 3-14, 2002, Vancouver, Canada.

[3] Alloy Digest, *Data on World Wide Metals and Alloys*, ARMCO 17-4 PH, Alloy Digest Inc. 1989.

[4] Winter, G., Nilson A.H., *Design of Concrete Structures*, 9th Edition, McGraw Hill Book Company, 1979.

[5] Conway, J.B., Stentz, R.H. and Berling, J.T., *Fatigue, Tensile and Relaxation Behaviour of Stainless Steels*, TID-26135, Technical Information Centre, Office of Information Services, United States Atomic Energy Commission, 1975.

[6] Bangash, M.Y.H., *Concrete and Concrete Structures: Numerical Modelling and Applications*, Middlesex Polytechnic, Faculty of Engineering, Science and Mathematics, London, New York, Elsevier Applied Science, 1989.

[7] Reinhold Publishing, *Materials Selector 75*, Volume 80 No. 4, September 1974.